for risk analysis. Finally, a randomized controlled trial is needed for further verification of the efficacy of JVD.

Recent studies have reported the utility of the combined use of JVD and deep dermal sutures in the obstetrics field.[16,17] However, based on the results from the present study, JVD and staples alone are sufficient for appropriate management of surgical wounds. Nevertheless, a randomized controlled trial considering factors, such as surgical procedure, subcutaneous fat-tissue closures, deep dermal sutures, use of antibiotics, and deep subcutaneous fat thickness, is necessary. Deep dermal sutures result in less postoperative pain for patients; compared to staples, they can maintain wound tension for a longer period. As such, deep dermal sutures are superior and should be recommended. However, deep dermal sutures take time to perform and need a certain amount of technique, which is a drawback.

The use of JVD incurs 637 health insurance points (material cost: 6370 yen). In contrast, the cost of a JVD in this hospital is 8138 yen (drain [6746 yen] + bag [1392 yen]). The difference between the health insurance points of the JVD and its cost to the hospital is 1738 yen, which incurs a cost loss for the hospital. In conclusion, this study revealed that subcutaneous JVD is useful for the closure of surgical incisions in gynecology and obstetrics, and that there are no limitations to their applicability.

Acknowledgments

We gratefully acknowledge all the members of the Department of Obstetrics and Gynecology, Kousei General Hospital.

Disclosure

None of the authors has anything to disclose.

References

1. Pitkin RM. Abdominal hysterectomy in obese women. *Surg Gynecol Obstet* 1976; **142**: 532–536.
2. Soper DE, Bump RC, Hurt WG. Wound infection after abdominal hysterectomy: Effect of the depth of subcutaneous tissue. *Am J Obstet Gynecol* 1995; **173**: 465–471.
3. Cardosi RJ, Drake J, Holmes S *et al.* Subcutaneous management of vertical incisions with 3 or more centimeters of subcutaneous fat. *Am J Obstet Gynecol* 2006; **195**: 607–616.
4. Berghella V, Baxter JK, Chauhan SP. Evidence-based surgery for cesarean delivery. *Am J Obstet Gynecol* 2005; **193**: 1607–1617.
5. Loong RL, Rogers MS, Chang AM. A controlled trial on wound drainage in caesarean section. *Aust N Z J Obstet Gynaecol* 1988; **28**: 266–269.
6. Allaire AD, Fisch J, McMahon MJ. Subcutaneous drain vs. suture in obese women undergoing cesarean delivery. A prospective, randomized trial. *J Reprod Med* 2000; **45**: 327–331.
7. Magann EF, Chauhan SP, Rodts-Palenik S, Bufkin L, Martin JN Jr, Morrison JC. Subcutaneous stitch closure versus subcutaneous drain to prevent wound disruption after cesarean delivery: A randomized clinical trial. *Am J Obstet Gynecol* 2002; **186**: 1119–1123.
8. Al-Inany H, Youssef G, Abd ElMaguid A, Abdel Hamid M, Naguib A. Value of subcutaneous drainage system in obese females undergoing cesarean section using Pfannenstiel incision. *Gynecol Obstet Invest* 2002; **53**: 75–78.
9. Ramsey PS, White AM, Guinn DA *et al.* Subcutaneous tissue reapproximation, alone or in combination with drain, in obese women undergoing cesarean delivery. *Obstet Gynecol* 2005; **105**: 967–973.
10. Ochsenbein-Imhof N, Huch A, Huch R, Zimmermann R. No benefit from post-caesarean wound drainage. *Swiss Med Wkly* 2001; **131**: 246–250.
11. Gallup DC, Gallup DG, Nolan TE, Smith RP, Messing MF, Kline KL. Use of a subcutaneous closed drainage system and antibiotics in obese gynecologic patients. *Am J Obstet Gynecol* 1996; **175**: 358–362.
12. Del Valle GO, Combs P, Qualls C, Curet LB. Does closure of Camper fascia reduce the incidence of post-cesarean superficial wound disruption? *Obstet Gynecol* 1992; **80**: 1013–1016.
13. Cetin A, Cetin M. Superficial wound disruption after cesarean delivery: Effect of the depth and closure of subcutaneous tissue. *Int J Gynaecol Obstet* 1997; **57**: 17–21.
14. Chelmow D, Huang E, Strohbehn K. Closure of the subcutaneous dead space and wound disruption after cesarean delivery. *J Matern Fetal Neonatal Med* 2002; **11**: 403–408.
15. Hellums EK, Lin MG, Ramsey PS. Prophylactic subcutaneous drainage for prevention of wound complications after cesarean delivery: a metaanalysis. *Am J Obstet Gynecol* 2007; **197**: 229–235.
16. Johnson A, Young D, Reilly J. Caesarean section surgical site infection surveillance. *J Hosp Infect* 2006; **64**: 30–35.
17. Inotsume-Kojima Y, Uchida T, Abe M, Doi T, Kanayama N. A combination of subcuticular sutures and a drain for skin closure reduces wound complications in obese women undergoing surgery using vertical incisions. *J Hosp Infect* 2011; **77**: 162–165.

BMC Cancer

RESEARCH ARTICLE Open Access

MicroRNA-21 is a candidate driver gene for 17q23-25 amplification in ovarian clear cell carcinoma

Yukihiro Hirata[1,2], Noriyuki Murai[2], Nozomu Yanaihara[1*], Misato Saito[1], Motoaki Saito[1], Mitsuyoshi Urashima[3], Yasuko Murakami[2], Senya Matsufuji[2] and Aikou Okamoto[1]

Abstract

Background: Epithelial ovarian cancer (EOC) is the most common cause of gynecological malignancy-related mortality. Ovarian clear cell carcinoma (CCC) has unique clinical characteristics and behaviors that differ from other histological types of EOC, including a frequent association with endometriosis and a highly chemoresistant nature, resulting in poor prognosis. However, factors underlying its malignant behavior are still poorly understood. Aberrant expression of microRNAs has been shown to be involved in oncogenesis, and *microRNA-21* (*miR-21*) is frequently overexpressed in many types of cancers. The aim of this study was to investigate the role of *miR-21* in 17q23-25 amplification associated with CCC oncogenesis.

Methods: We identified 17q23-25 copy number aberrations among 28 primary CCC tumors by using a comparative genomic hybridization method. Next, we measured expression levels of the candidate target genes, *miR-21* and *PPM1D*, for 17q23-25 amplification by real-time RT-PCR analysis and compared those data with copy number status and clinicopathological features. In addition, immunohistochemical analysis of PTEN (a potential target of *miR-21*) was performed using the same primary CCC cases. We investigated the biological significance of *miR-21* overexpression in CCC using a loss-of-function antisense approach.

Results: 17q23-25 amplification with both *miR-21* overexpression and PTEN protein loss was detected in 4/28 CCC cases (14.2%). The patients with 17q23-25 amplification had significantly shorter progression-free and overall survival than those without 17q23-25 amplification (log-rank test: $p = 0.0496$; $p = 0.0469$, respectively). A significant correlation was observed between *miR-21* overexpression and endometriosis. Both *PTEN* mRNA and PTEN protein expression were increased by *miR-21* knockdown in CCC cells. We also confirmed that *miR-21* directly bound to the 3′-untranslated region of *PTEN* mRNA using a dual-luciferase reporter assay.

Conclusions: *MiR-21* is a possible driver gene other than *PPM1D* for 17q23-25 amplification in CCC. Aberrant expression of *miR-21* by chromosomal amplification might play an important role in CCC carcinogenesis through the regulation of the *PTEN* tumor suppressor gene.

Keywords: Ovarian clear cell carcinoma, CGH array, microRNA-21, PTEN

Background

Epithelial ovarian cancer (EOC), a heterogeneous group of neoplastic diseases that arise from the epithelial cells of fallopian tubes, ovarian fimbria, ovarian surface epithelium, inclusion cysts, peritoneal mesothelium, or endometriosis, is the most lethal gynecologic malignancy in western countries and in Japan [1]. EOC can be classified into four major histological types: serous, mucinous, endometrioid adenocarcinoma, and clear cell carcinoma (CCC). CCC has unique clinical characteristics that differ from other histological types of EOC. CCC accounts for 5–25% of all EOC, depending on the population. The prevalence of CCC among EOCs in North America and Europe is 1–12%, while that in Japan is approximately 20% [2]. CCC is frequently associated with coexistent endometriosis and thrombosis, with 20% of patients

* Correspondence: yanazou@jikei.ac.jp
[1]Department of Obstetrics and Gynecology, The Jikei University School of Medicine, 3-25-8, Nishi-Shinbashi, Minato-ku, Tokyo 105-8461, Japan
Full list of author information is available at the end of the article

developing deep venous thrombosis. Endometriosis has been identified in more than 30% of tumors and is reported to be a precursor of CCC as well as endometrioid adenocarcinoma [3]. The incidence of venous thromboembolic events was found to be significantly higher in CCC than in other epithelial ovarian cancers [4,5]. A greater proportion of CCC presents in the early stage as a large pelvic mass, which may account for their earlier diagnosis. However, CCC is generally refractory to standard platinum agent-based chemotherapy with a response rate of only 11–15%; therefore, this type of tumor typically has a poor prognosis, particularly in late stages. The survival rates of patients with CCC are significantly lower than those of patients with serous EOC [6]. Identifying novel therapeutic targets and establishing new treatment strategies for CCC is thus important.

The common molecular genetic alterations identified so far in CCC include mutations in *ARID1A* and *PI3K* as well as HNF1B overexpression. However, the molecular landscape of CCC oncogenesis remains poorly understood [7,8]. Since chromosomal aberrations are a cardinal feature of carcinogenesis, the identification of amplified or deleted chromosomal regions associated with CCC would elucidate its underlying pathogenetic mechanisms. Amplification at chromosome17q23-25 has been reported to occur with a frequency of approximately 40% in CCC [9]. The *PPM1D* gene (also known as *WIP1*) maps to the 17q23.2 amplicon and is amplified and/or overexpressed in various types of cancers, including CCC [10]. However, the frequency of *PPM1D* overexpression in CCC is reported to be only about 10%. In addition, the peak region of 17q23-25 amplification in CCC as assessed by GISTIC analysis maps adjacent to the *PPM1D* locus. Taken together, these findings suggest the involvement of undiscovered driver genes on 17q23-25 in CCC [11].

Recent evidence has shown that microRNAs (miRNAs) can have oncogenic or tumor suppressor functions and contribute to cancer biology [12,13]. Aberrant expression of miRNAs has been shown to be associated with oncogenesis. One of the most frequently overexpressed miRNAs in many types of cancers is *miRNA-21*, located on 17q23.2 within the intron of the *TMEM49* gene [14]. Protein expression of the *PTEN* gene, a target gene of *miR-21* [15], is absent in one-third of all CCC cases [16,17]. We thus hypothesized that *miR-21* is a potential candidate for 17q23-25 amplification and might play an important role in CCC oncogenesis through the regulation of PTEN expression.

Methods

Clinical specimens and ovarian cancer cell cultures

Tissue specimens were obtained from 28 patients with ovarian CCC who were treated at Jikei University Hospital from 2000 to 2010. The Jikei University School of Medicine Ethics Review Committee approved the study protocol (ethics approval number: 14-132) and informed consent was obtained from all patients. Most patients (27 of 28) underwent surgical resection followed by adjuvant chemotherapy with platinum-based regimens (platinum/paclitaxel, n = 12; platinum/irinotecan hydrochloride, n = 13; docetaxel/carboplatin, n = 2) as initial treatment. None of the patients had received chemotherapy or radiation therapy before the initial surgery. All samples were examined as hematoxylin–eosin-stained sections by a pathologist to confirm pure CCC histologically. Tumors were classified according to the World Health Organization classification system, and clinical stages were determined using the International Federation of Gynecology and Obstetrics (FIGO) staging system. Progression-free survival (PFS) was defined as the time from the date of primary surgery to the date of disease progression. Overall survival (OS) was calculated for the time from the date of initial surgery to the last follow-up visit or death. The mean age was 53 years (range, 37–81). FIGO staging was as follows: Stage I, n = 18; stage II, n = 2; stage III, n = 8. The median follow-up period was 45.7 months (range, 5.1–99.3). Coexistent endometriosis was found in 20 (71.4%) of 28 patients. The ovarian CCC cell lines JHOC-5 and JHOC-9 were obtained from Riken Bioresource center (Tsukuba, Japan). HAC-2 was kindly provided by Dr. Nishida (Tsukuba University, Ibaraki, Japan). RMG-I and RMG-II were provided by Dr. D. Aoki (Keio University, Tokyo, Japan). HAC-2, JHOC-5, and JHOC-9 cells were cultured in RPMI-1640 medium (Sigma-Aldrich, Tokyo, Japan). RMG-I and RMG-II were cultured in Ham F-12 medium (Sigma-Aldrich). Both media contained 10% heat inactivated fetal bovine serum, Penicillin-Streptomycin-Amphotericin B Suspension (×100) (Wako, Osaka, Japan). Cells were incubated at 37°C in a humidified atmosphere containing 5% CO_2.

DNA and RNA isolation

All surgical samples were composed of at least 80% neoplastic cells and were immediately frozen after collection. For RNA isolation, the fresh clinical specimens were stored at 4°C for 24 hours in RNAlater (Ambion, Austin, Texas, USA) and were then frozen at −80°C in liquid nitrogen until further use. Using a commercially available DNA isolation kit (GentraPureGene kit; Qiagen, Tokyo, Japan), genomic DNA was extracted from stored frozen tumor samples following the manufacturer's instructions. Total RNA was isolated from tumor samples and cell lines with Trizol reagent (Invitrogen, Carlsbad, CA, USA), according to the manufacturer's instructions. Total RNA from the tumor samples was stored in RNAlater.

Candidate gene selection

Array comparative genomic hybridization (aCGH)

For this validation study, aCGH was performed using the Agilent Human Genome CGH 244AMicroarray Kit

244 K (Agilent Technologies, Santa Clara, CA, USA). DNA digestion, labeling, and hybridization were performed as recommended by the manufacturer. The test DNA (2 μg) and reference DNA (2 μg) were digested with Rsa I and Alu I (Promega). The digested tumor DNA and reference DNA were labeled with either cyanine (Cy) 5-deoxyuridine triphosphate (dUTP) or Cy3-dUTP using the Agilent Genomic DNA Labeling Kit PLUS (Agilent Technologies). Labeled DNAs were purified using Microcon YM-30 filters (Millipore, Billerica, MA, USA). The hybridization mixture, containing Cy3-labeled test DNA and Cy5-labeled reference DNA, 2× Hybridization buffer (Agilent), 10× blocking agent (Agilent), and Human Cot-1 DNA (Invitrogen), was prepared in an Agilent SureHyb chamber. All microarray slides were scanned on the Agilent Microarray Scanner G2505B. Date was obtained using Feature Extraction software, version 10.7.3.1 (Agilent Technologies). Penetrance of aberrant chromosomal areas across the genome was demonstrated using Aberration Detection Method 2 (Agilent Genomic Workbench Lite Edition 6.5.0.18, Agilent Technologies), a quality-weighted interval score algorithm that identifies aberrant intervals in samples that have consistent gain or loss log ratios based on their statistical score. The $\log_2$ ratios for whole chromosomal number changes that were completely gained, lost, or had no change were evaluated. The threshold for determining amplification or deletion was defined as $\log_2$ ratio >0.5 or < −0.5.

Copy number assay for region 17q23–25 in the miR21 gene in CCC cells

The copy number for the 17q23–25 region was determined using commercially available and custom TaqMan Copy Number Assays (Applied Biosystems, Foster City, CA, USA). The *TERT* locus was used as an internal reference copy number. Genomic DNA was extracted from CCC cell lines (HAC-2, JHOC-5, JHOC-9, RMG-I, and RMG-II) using commercially available gDNA extraction and purification kits. Real-time genomic PCR was performed in a total volume of 20 μL per well containing TaqMan genotyping master mix (10 μL), genomic DNA (20 ng), and primers (20 ng each). Data were analyzed using SDS 2.2 sand CopyCaller software (Applied Biosystems). Copy numbers were assigned as follows: actual copy number <0.5, assigned copy number 0 (gene deletion); actual copy number ≥0.5 but <1.5, assigned copy number 1; actual copy number ≥1.5 but <2.5 , assigned copy number 2; actual copy number ≥2.5 but <3.5, and assigned copy number 3.

Quantitative reverse transcription-polymerase chain reaction

Reverse transcription (RT) of *miR-21* was carried out using the Taqman microRNA reverse transcription kit (Applied Biosystems, Foster City, CA, USA). cDNAs were synthesized from 2 μg of total RNA using the Superscript cDNA Synthesis Kit (Invitrogen) for *PPM1D* and *PTEN* mRNA detection. Real-time PCR Reactions with TaqMan Fast Advanced Master Mix (Applied Biosystems) were performed in 96-well plates using the Applied Biosystems StepOnePlus Real-time PCR System (Applied Biosystems). Each reaction was analyzed in triplicate. *MiR-21* expression was normalized to that of *U6* small nuclear RNA, and *PPM1D* and *PTEN* expression was normalized to that of *GAPDH*. The expression of *miR-21*, *PPM1D*, and *PTEN* were defined based on the threshold cycle (Ct); relative expression levels are presented as $2^{-\Delta\Delta Ct}$.

Immunohistochemical analysis

Immunohistochemical analysis of PTEN expression (1:100 dilution, Cell Signaling Technologies) was performed on 3-μm paraffin sections of formalin-fixed, paraffin-embedded tissues using the Ventana Discovery XT automated stainer (Ventana Medical Systems, Tucson, AZ, USA). After deparaffinization, antigen retrieval was carried out in CC1 buffer (Cell Conditioning 1; citrate buffer pH 6.0, Ventana Medical Systems). PTEN expression was scored independently by two investigators (Y. H. and N. Y.) based on stain intensity and extent. Immunohistochemical scoring was conducted in a manner entirely blinded to all clinical and biological variables. The intensity of positive staining was scored from 0 to 2 as follows: 0 (none), 1 (weak; intensity < positive control), 2 (strong; intensity ≥ positive control). Positive staining was assigned using a semi-quantitative, five-category grading system: 0, <5% positive cells; 1, 6–25% positive cells; 2, 26–50% positive cells; 3, 51–75% positive cells; 4, 76–100% positive cells. Addition of the two values gives the total score, and a score <4 was considered PTEN-negative.

Additional cohort

Additional cohort study was also approved by The Jikei University School of Medicine Ethics Review Committee (ethics approval number: 14-132). An additional cohort was analyzed using aCGH, realtime-PCR, and immunohistochemistry. This additional cohort was included to ensure association between miR21 overexpression and PTEN protein loss using 43 patients, with further confirmation in an additional 15 patients.

Western blot analysis

Western blot analysis was performed to detect PTEN protein expression (dilution of 1:2000, Cell Signaling Technologies, Danvers, MA, USA). CCC cell lines were washed in PBS and lysed in RIPA buffer containing 200 mM Tris-HCl (pH 7.2), 150 mM NaCl, 0.1% SDS, 1% Nonidet P-40, 1% sodium deoxycholate, 2 mM EDTA, 50 mM NaF, 1% proteinase inhibitors, and 1% PMSF for 10 min on ice. Cell lysates were then sonicated

for 30 seconds, and cellular debris were removed by centrifugation at 14 000 rpm at 4°C for 30 min. Supernatants were collected and assayed for protein concentration using the BCA Protein Assay Kit (Invitrogen). Supernatants containing an equal amount of protein extract were supplemented with concentrated 4× LDS sample buffer (Invitrogen) and heated at 95°C for 5 min. Approximately 40 μg of lysate was loaded onto a 12.5% SDS-polyacrylamide gel. The supernatants were separated by SDS–PAGE, and proteins were transferred to Immobilon-P transfer membrane (Millipore, Milford, MA, USA). The transfer membrane was incubated with primary antibody in TBS with 0.1% Tween-20 and 5% bovine serum albumin overnight at 4°C. Anti-rabbit IgG-conjugated horseradish peroxidase (GE Healthcare) was used as the secondary antibody. The transfer membrane was incubated with secondary antibody in TBS with 0.1% Tween-20 and 5% skim milk for 90 min at room temperature. The proteins were visualized using the ECL-Plus Western blotting detection system and detected using the Image Quant LAS 4000 mini (GE Healthcare). The concentration of each target protein was normalized against beta-actin.

Transfection

Twenty four hours before transfection, cells were seeded in plates and grown to 50% confluence. For inhibition of miR-21, RMG-II cells were transfected with *mir*Vana miRNA Inhibitors or a control (Ambion). Transfections were performed using Lipofectamine RNAiMAX (Invitrogen) according to the manufacturer's protocol.

Dual luciferase reporter assay

pGL3 wild-type *PTEN* 3′-UTR and pGL3 mutant-type *PTEN* 3′-UTR luciferase plasmids were obtained from Addgene (Cambridge, MA). RMG-II cells were seeded in 6-well plates (5×105 cells/well). After 24 h, the cells were transfected with pGL3 control vector (Promega), pGL3 wild-type *PTEN* 3′-UTR vectors, or pGL3 mutant-type *PTEN* 3′-UTR vectors using Lipofectamine 2000 reagent. Luciferase activities were measured using the Dual-Luciferase Reporter Assay system (Promega) 24 h after transfection. Firefly luciferase activity was normalized to renilla activity for each sample. All the experiments were performed in triplicate.

MTS assay

MTS assay was performed using the CellTiter 96 AQueous One Solution Cell Proliferation Assay kit (Promega, Madison, WI, USA) following the manufacturer's protocol. Briefly, miR-21 inhibitor and negative control oligonucleotides were transfected at a final concentration of 200nM. After 24 hours transfection, RMG-II cells were seeded into 96-well plates at a density of 1×10^4 cells per well. MTS (20 μL) was added to each well 3 hours before the desired time points, and cells were incubated at 37°C. The absorbance was measured at 490 nm using a Microplate Reader (VersaMAx, Molecular Devices). All experiments were repeated three times. Values are presented as the mean ± standard deviation (SD).

Invasion assay

Cells were seeded into the top chamber of a 96-well matrigel-coated plate with 8-μm-pore polyethylene terephthalate membrane inserts (Corning). MiR-21 inhibitor and negative control oligonucleotides were transfected at a final concentration of 200nM.The bottom chamber was filled with 0.75 mL Ham F-12 medium with 10% FBS as a chemoattractant. The inserts were filled with 0.5 mL Ham F-12 medium with 1% FBS. After incubation for 48 h, the filter membrane was fixed with 100% methanol and stained with hematoxylin and eosin. The degree of invasiveness was quantified by counting the number of cells in 4 random fields of view per filter using 400× magnification. Data obtained from three separate inserts are shown as mean values.

Statistical analysis

All statistical analyses were performed using StatMate III software (ATMS, Tokyo, Japan). Comparisons between parameters were made using Fisher's exact test. For survival analysis, PFS and OS distributions were determined using the Kaplan–Meier method, and the resulting curves were compared using the log-rank test. $P < 0.05$ was considered statistically significant.

Results

Chromosome 17q23-25 amplification, miR-21 expression, and PTEN protein expression in CCC

CGH array profiles of chromosome 17 in 28 primary CCCs revealed that 9 out of 28 patients (32%) showed 17q23-25 amplification that included *miR-21* (Figure 1). *MiR-21* and *PPM1D* mRNA expression were then measured by real-time RT-PCR analysis (Additional file 1: Figure S1). We defined standardized value as each median value of *miR-21* and *PPM1D* expression without 17q23-25 amplification. Overexpression of *miR-21* and *PPM1D* were found in 60% and 57% of these tumors, respectively. Seven of 9 tumors (77.7%) with 17q23-25 amplification showed *miR-21* overexpression, and 10 of 19 tumors (52.6%) without 17q23-25 amplification also showed *miR-21* overexpression. In addition, 6 of 9 tumors (66.6%) with 17q23-25 amplification showed *PPM1D* overexpression, and 10 of 19 tumors (52%) without 17q23-25 amplification showed *PPM1D* overexpression (Additional file 1: Figure S1). We next evaluated the relationship between 17q23-25 amplification and either *miR-21* or *PPM1D* overexpression. No significant correlation between

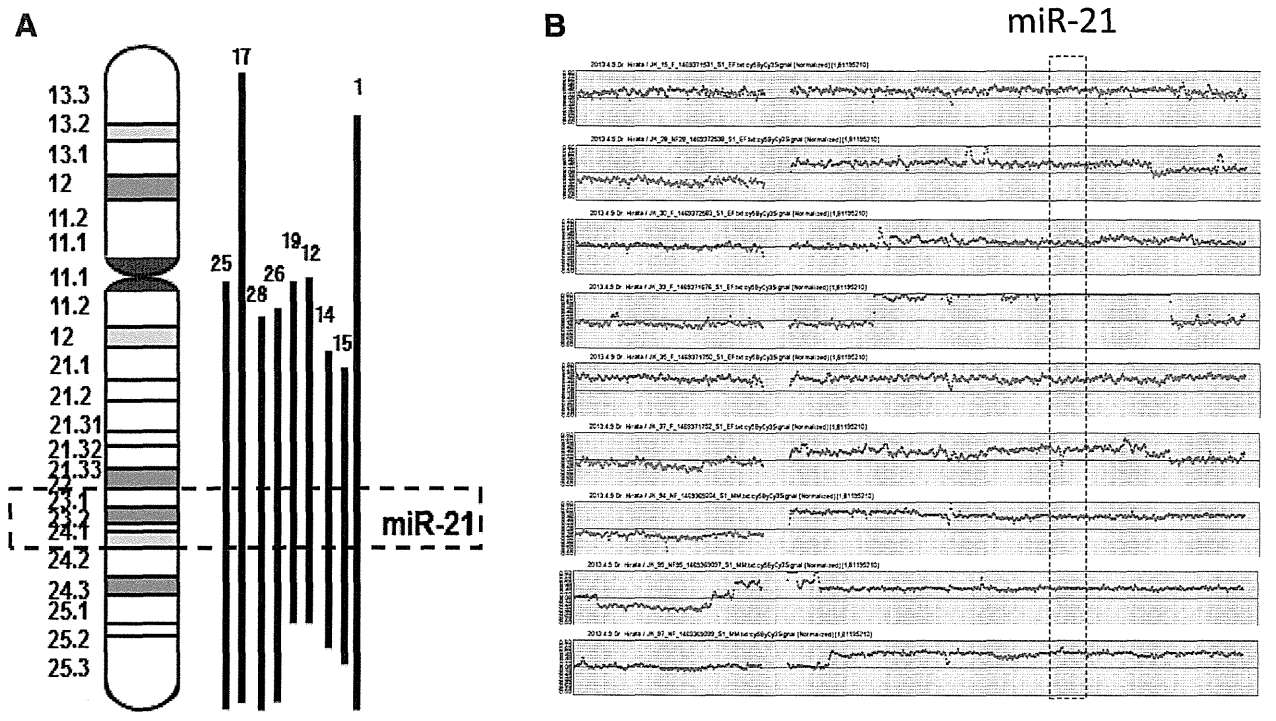

Figure 1 Frequency of copy number changes in chromosome 17 by array CGH in 28 CCC. (A) chromosome 17 is represented by ideograms showing G-banding patterns. Bold vertical lines on the ideogram indicate the region of chromosomal amplification. The number at the top of each line represents the primary tumor in which the indicated change was recorded. Nine samples showed 17q23-25 amplification that included miR-21. **(B)** The gains and losses are shown as green and red color bars, respectively. These samples showed 17q23-25 amplification that included miR-21.

the amplification and overexpression was observed for either gene. Next, immunohistochemical analysis of PTEN (a potential target of *miR-21*) was performed on samples from the same primary CCC patients. Loss of PTEN protein was observed in 13 of 28 patients (46.4%) (Additional file 2: Figure S2) and in 6 of 17 tumors (35.3%) with *miR-21* overexpression. No significant correlation was observed between *miR-21* overexpression and loss of PTEN expression. To further confirm these results, we added 15 CCC samples from an additional cohort, performing real-time RT-PCR of miR21 and IHC of PTEN. Again, no significant correlation was observed between *miR-21* overexpression and loss of PTEN expression (date not shown). In total, as shown in Figure 2, the occurrence of 17q23-25 amplification with both *miR-21* overexpression and PTEN protein loss was detected in 4 out of 28 CCC patients (14.2%) (Figure 2).

Associations between clinicopathological parameters and either 17q23-25 amplification, miR-21 overexpression, or PTEN protein loss

The relationship between clinicopathological parameters and genetic alterations including 17q23-25 amplification, *miR-21* overexpression, and decreased PTEN protein expression are summarized in Table 1. Interestingly, a significant correlation was observed between *miR-21* overexpression and endometriosis. Meanwhile, no correlations were observed between the other clinical parameters and any of the genetic alterations. According to survival analysis, patients with 17q23-25 amplification had significantly shorter progression-free and overall survival times than did those without 17q23-25 amplification (log-rank test; PFS, p = 0.0496; OS, p = 0.0469) (Table 2). On the other hand, the PFS and OS did not correlate significantly with *miR-21* overexpression or PTEN protein loss.

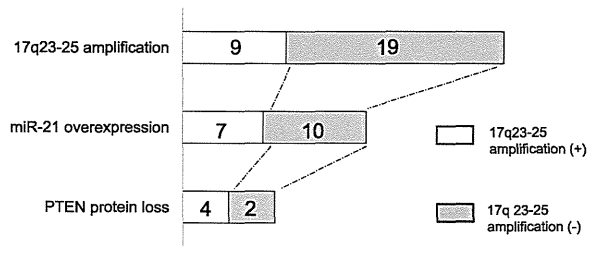

Figure 2 Analysis of clinical CCC specimens. Of the 9 tumors with 17q23-25 amplification, 7 (77.7%) showed *miR-21* overexpression. Of the 19 tumors (58.8%) without 17q23-25 amplification, 10 showed *miR-21* overexpression. Of all the 28 17q23-25 amplification cases, both *miR-21* overexpression and PTEN protein loss were detected in 4 (14.2%).

Table 1 Associations between clinicopathological parameters and either 17q23-25 amplification, *miR-21* overexpression, or PTEN protein loss

Variable	Cases (Total 28)	17q23-25 amplification		*miR-21* overexpression		Loss of PTEN protein expression	
		n = 9	P value	n = 17	P value	n = 13	P value
Age	6			4	>0.9999	5	0.0690
≧60	22	2	>0.9999	13		8	
< 60		7					
Stage			0.6464		>0.9999	8	0.1977
I-II	21	6		11		5	
III-IV	7	3		4			
Lymph node status	7				>0.9999	4	0.6702
Metastasis	21	3	0.6219	4		9	
No metastasis		6		11			
Endometriosis		8	0.2143	15		10	0.6859
Positive	20	1		2	0.0298	3	
Negative	8						
Thrombosis	3	1	>0.9999	2	>0.9999	2	0.5833
Positive	25	8		13		11	
Negative							

No correlations were observed between the other clinical parameters (age, stage, lymph node metastasis, thrombosis, and either 17q23-25 amplification, *miR-21* overexpression, or PTEN protein loss). A significant correlation was observed between *miR-21* overexpression and endometriosis. P-values were from two-sided tests and statistically significant when <0.05.

MiR-21 modulates PTEN expression

Based on the profiles of 17q23-25 copy number changes, *miR-21* expression, *PTEN* mRNA expression, and PTEN protein expression in 5 CCC cell lines, we selected RMG-II cells for further functional analysis. We considered this cell line to be ideal because the cells showed relatively 17q23-25 amplification, high *miR-21* expression with decreased PTEN protein expression (Additional file 3: Figure S3 and Additional file 4: Figure S4).

To investigate the regulation of PTEN expression by *miR-21* in CCC, we used a loss-of-function antisense approach in RMG-II cells. Knockdown efficiency was confirmed by real-time RT-PCR analysis of *miR-21* (Figure 3A). In RMG-II cells, we found that *miR-21* knockdown caused a significant increase in PTEN protein expression as indicated by Western blot analysis, along with increased *PTEN* mRNA expression (Figure 3A). However, suppression of *miR-21* expression did not inhibit cell proliferation or invasion (date not shown). We next investigated the direct binding of *miR-21* to the 3'UTR of PTEN mRNA by luciferase assay using a pGL3 plasmid harboring either the wild- or mutant-type *PTEN* 3'-UTR. The activity of the luciferase reporter was significantly decreased when fused to the wild-type *PTEN* 3′-UTR. Deletion mutations in the *miR-21*–interacting seed region rescued the luciferase activity. Taken together, these data suggest that *PTEN* is a direct functional target of

Table 2 Proportional hazard regression analysis of single predictors for PFS and OS in CCC

Parameters	PFS		OS	
	95%CI	P-value	95%CI	P-value
Age (≦60 vs. >60 years)	0.289–1.656	0.3371	0.244–-1.965	0.3337
Stage (I, II vs. III, IV)	0.289–1.234	<0.05	0.289–1.168	<0.05
Endometriosis	0.153–2.834	0.2384	0.154–2.684	0.2156
Residual tumor ≦2 VS. >2 cm)	0.3440–2.484	<0.05	0.1332–2.408	<0.05
17q23-25 amplification	0.1768–1.684	0.0496	0.154–1.756	0.0469
miR-21 overexpression	0.441–1.168	0.3141	0.441–1.645	0.3204
PTEN protein loss	0.4422–1.980	0.6393	0.3771–1.465	0.7067

PFS, progression-free survival; OS, Overall survival; CI, Confidence interval.
For survival analysis, PFS and OS distribution was determined using the Kaplan–Meier method. The patients with 17q23-25 amplification had significantly shorter PFS and OS than that did those without 17q23-25 amplification in CCC tumors Meanwhile, PFS and OS did not show significant correlations in *miR-21* overexpression, PTEN protein loss, or clinicopathological date.

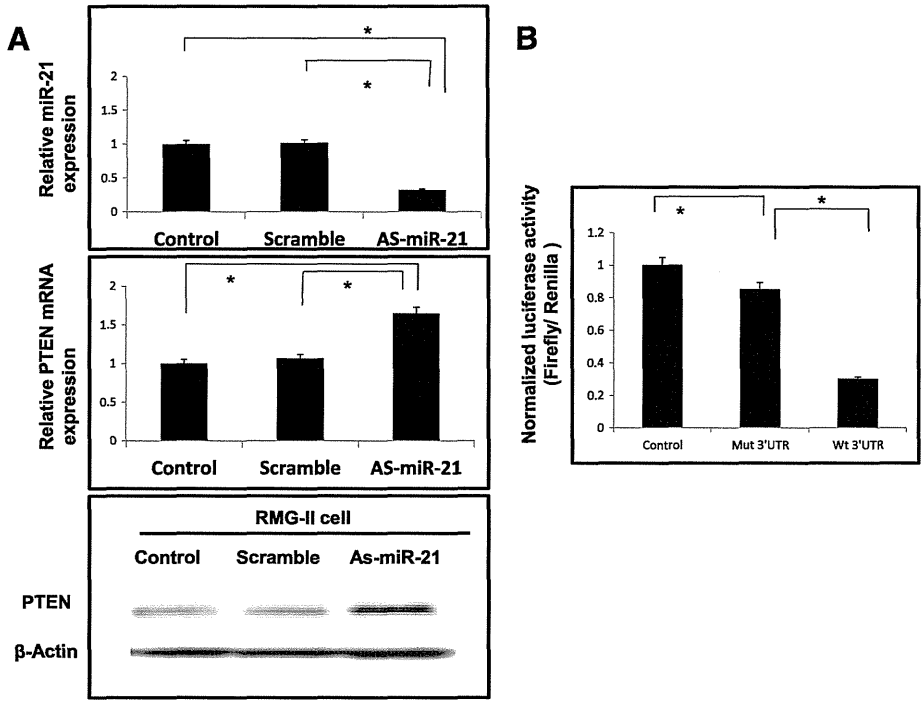

Figure 3 *miR-21* modulates PTEN tumor suppressor gene expression. To evaluate the biological significance of *miR-21* overexpression in CCC, we used a loss-of-function antisense approach. An antisense *miR-21* oligonucleotide (ODN) was used to knock down *miR-21* expression in RMG-II cells. **(A)** Efficiency of RMG-II cell transfection was confirmed by real- time RT PCR. *PTEN* mRNA expression was increased by knockdown of *miR-21* in RMG-II cells. Western blot analysis showing that PTEN expression was increased in RMG-II cells upon inhibition of *miR-21*. **(B)** *MiR-21* directly targets the 3'-UTR of *PTEN* mRNA. The activity of luciferase in the pGL3 wild-type *PTEN* 3'-UTR was downregulated compared to pGL3 mutant-type *PTEN* 3'-UTR and the pGL3 control in RMG-II cells. P <0.05 according to the t-test.

miR-21, and its expression is regulated by *miR-21* in CCC (Figure 3B). Several potential miR21 targets that could have implications in CCC were identified using web-based computational approaches to predict gene targets (miRBase Targets BETA Version 1.0, PicTar predictions, and TargetScan). Three putative target genes, PDCD4, SMARCA4, and SPRY2, were predicted by 3 different programs. This result indicates that tumor suppressor genes are potentially regulated by miR21. Therefore, we performed real-time RT-PCR for PDCD4, SMARCA4, SPRY2 in the miR21 knockdown experiments in RMG-II cells. We found that *miR-21* knockdown increased the expression of these mRNAs (Additional file 5: Figure S5). To investigate the regulation of PTEN expression by *miR-21* in JHOC9 cells, we overexpressed miR21 using miR21 mimics in JHOC9 cell. Quantitative real-time PCR analysis confirmed the level of miR21 was significantly overexpressed. As expected, the level of PTEN mRNA was downregulated in JHOC9 cells. Expression of PDCD4, SMARCA4, and SPRY2 mRNA was also decreased by the overexpression of miR-21 in response to miR-21 mimics in JHOC9 cells (Additional file 6: Figure S6).

Discussion

DNA copy number aberrations are a frequent event in many malignant tumors, leading to altered expression and function of genes residing within the affected genome region. Such genomic abnormalities can harbor either oncogenes or tumor suppressor genes depending on the original gene function and whether the copy number is amplified or deleted. Previous studies have identified a high frequency of copy number amplifications in CCC, including 17q23-25 (18-40%), 20q13 (22-25%), and 8q21q- 24q. Additionally, deletions at chromosome 9q and 19p have been also reported in CCC [9,18-20]. Of the chromosomal alterations associated with CCC, 17q23-25 is one of the most frequently amplified regions and is reported to be associated with patient outcome [9]. So far, *PPM1D* and *APPBP2* have been identified as potential targets of 17q23-25 amplification in CCC. However, a recent report suggests there might be new driver genes other than *PPM1D* and *APPBP2* in this region [11]. More than half of miRNAs have been aligned to genomic fragile sites or frequently deleted or amplified regions in several malignancies [21,22]. MiRNAs are a class of small, non-coding RNA molecules that regulate gene expression

through translational repression or cleavage of target mRNA. Among them, *miR-21*, located on 17q23.2, is unique in that it is overexpressed in many cancers as an oncogene. Previous studies have revealed several significant *miR-21* targets that might be related to carcinogenesis. Based on this evidence, *miR-21* is a potential candidate for 17q23-25 amplification in CCC oncogenesis.

We analyzed DNA copy number alterations at chromosome 17 in a panel of 28 primary CCCs using CGH array. In our data set, 17q23-25 amplification was observed at a frequency similar to that of previous reports. In addition, we confirmed that 17q23-25 amplification correlated negatively with patient prognosis, suggesting that the chromosomal alteration might result in the overexpression of genes that contribute to the genomic instability of CCC. Although we did not find a statistical correlation between *miR-21* overexpression and amplification of this region, overexpression of *miR-21* was observed in 60% of the CCC cases examined.

Targets of *miR-21* in cancer include *PTEN*, *PDCD4*, *LRRFIP1*, *RECK*, *TIMP-3*, *TPM1*, *BTG2*, and *Sprty2* [23]. *PTEN* can restrict growth and survival signals by limiting the activity of the phosphoinositide 3-kinase (PI3K) pathway. A decrease in PTEN might cause activation of the PI3K pathway, including Akt and mTOR, which leads to tumor development [24]. The prominent role of PTEN inactivation in CCC is thought to involve multiple mechanisms. In our study, loss of PTEN protein was observed in 46% of CCC patients. On the other hand, low of PTEN copy number was not indicted by CGH array (data not shown). Furthermore, no significant correlation was observed between *miR-21* overexpression and loss of PTEN expression in our date set. Therefore, we suggest the involvement of another epigenetic mechanism, such as *PTEN* mutations, promoter methylation of *PTEN*, loss of heterozygosity at the *PTEN* locus other miR are infrequent in CCC. Although there was no statistical correlation between PTEN loss and *miR-21* overexpression, the occurrence of 17q23-25 amplification along with both *miR-21* overexpression and PTEN protein loss was detected in 14% of CCC cases. Thus, this oncogenetic mechanism might play a prominent role in CCC. Additionally, we showed that *miR-21* inhibition significantly increased PTEN expression in vitro. Moreover, the results obtained from the dual luciferase reporter assay supports the idea that *miR-21* directly targets the *PTEN* gene, regulating the protein expression. It is therefore possible that miRNAs such as *miR-21* modulate PTEN expression by transcriptional regulation or target degradation in CCC.

Finally, we found a significant correlation between *miR-21* overexpression and endometriosis in CCC. Endometriosis-related CCC is thought to be a chronic inflammatory disease, characterized by increased production of pro-inflammatory cytokines such as IL-1, IL-6, IL-8, IL-10, and TNF-α [25]. We recently reported that CCC showed a dominant Th-2 cytokine expression pattern driven largely by *IL-6* expression [26]. In addition, IL-6 induces *miR-21* expression through a STAT3-dependent pathway [27]. We also confirmed that IL-6 induces *miR-21* overexpression in RMG-II (data not shown). In our study, *miR-21* overexpression was observed in 60% of the CCC cases, regardless of 17q23-25 amplification status, suggesting another mechanism might regulate *miR-21* expression. *miR-21* might contribute to inflammation-induced

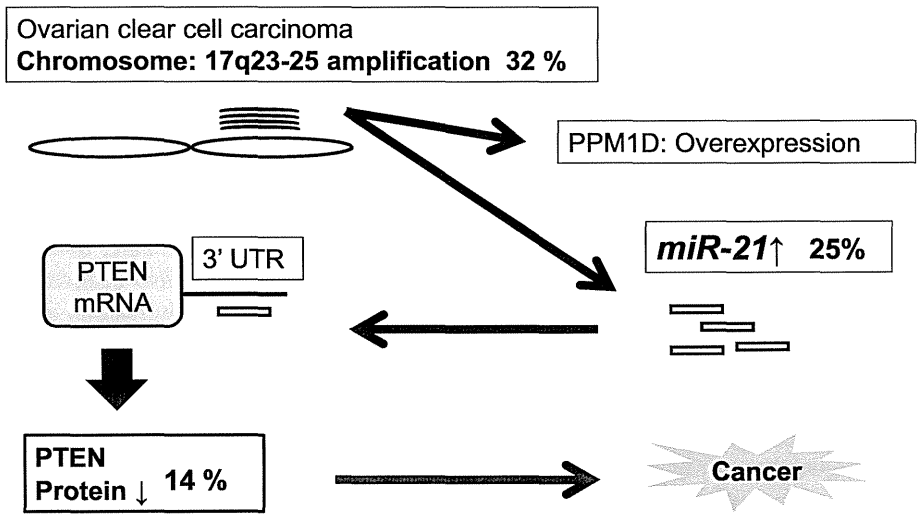

Figure 4 Chromosome 17q23-25 amplification, *miR-21* expression, and PTEN protein expression in CCC. CGH array was performed to evaluate chromosomal alterations in 28 primary CCC tumors. Nine out of 28 patients (32%) showed chromosomal amplification in the 17q23-25 region that contains *miR-21*. Seven of 9 tumors (77.7%) with 17q23-25 amplification showed *miR-21* overexpression. 17q23-25 amplification with both *miR-21* overexpression and PTEN protein loss was detected in 4/28 cases (14.2%).

carcinogenesis in CCC with endometriosis. We need to further analyze miR21 expression using in situ hybridization in the endometriotic lesions of CCC specimens. The correlation between miR21 and endometriosis observed in our study indicates a role for miR21 in precursor lesions of ovarian CCC.

Conclusions

This study is the first to indicate *miR-21* as the gene of interest in 17q23-25 amplification associated with CCC (Figure 4). Aberrant expression of *miR-21* by chromosomal amplification might play an important role in CCC carcinogenesis through regulating the *PTEN* tumor suppressor gene. Moreover, the modulation by *miR-21* overexpression of genes other than *PTEN* should not be overlooked in determining the oncogenic mechanism of CCC.

Additional files

Additional file 1: Figure S1. *MiR-21* and *PPM1D* mRNA expression located on 17q23- 25. Black dots indicate a cluster with 17q23-25 amplification, and white dots indicate a cluster without 17q23-25 amplification. We measured the median expression of *miR- 21* and *PPM1D* mRNA and set a transverse line as standard value. Seven of 9 tumors with 17q23-25 amplification showed *miR-21* overexpression. Six of 9 tumors with 17q23-25 amplification showed *PPM1D* overexpression.

Additional file 2: Figure S2. Immunohistochemical analysis of PTEN that might be a potential target of *miR-21* was performed using the same primary CCC cases. The intensity of positive staining was scored from 0 to 2, while the extent of positive staining was scored from 0 to 4. Addition of the two values gives the total score; scores >4 were considered PTEN-positive. (A) Typical image of a PTEN-negative case. (B) Typical image of a PTEN-positive case. Loss of PTEN protein was observed in 13 of 28 patients (46.4%).

Additional file 3: Figure S3. Frequency of copy number changes in Chr 17q23-25 region by copy number assay in 5 CCC cell lines. We found the copy number was increased in RMG-I and RMG-II cells.

Additional file 4: Figure S4. *MiR-21*, *PTEN* mRNA, and PTEN protein expression in CCC cell lines. (A) (B) Relative expression of *miR-21* and *PTEN* mRNA were detected with real-time RT-PCR, and the relative amount of *miR-21* was determined using $2^{-\Delta\Delta}CT$. (C) PTEN protein was measured by western blotting. The RMG-II cell line was selected for further analysis, because it had the most prominently overexpressed *miR-21* and decreased PTEN protein of the CCC cell lines.

Additional file 5: Figure S5. Three putative target genes, PDCD4, SMARCA4, and SRY2, are potentially regulated by miR21. (A) (B) (C) Real-time RT-PCR for PDCD4, SMARCA4, SPRY2 in the miR21 knockdown experiments in RMG-II cells. *miR-21* knockdown caused an increase in mRNA expression of these genes by real-time RT PCR in RMG-II cells.

Additional file 6: Figure S6. Mir21 modulates PTEN expression in JHOC9 cell. To investigate the regulation of PTEN expression by *miR-21* in JHOC9 cells, we overexpressed miR21 by miR21 mimics in JHOC9 cells. Quantitative real-time PCR analysis confirmed miR21 was significantly overexpressed. As expected, the level of PTEN mRNA was downregulated in JHOC9 cells. PDCD4, SMARCA4, and SRY2 mRNAs were also reduced by the overexpression of miR-21 in response to miR-21 mimics in JHOC9 cells.

Competing interests

The authors declare that they have no competing interests.

Authors' contributions

YH performed experiments and analyzed data. YH and NY drafted manuscript YH, MU, and AO carried out bioinformatics analyses of the CGH data. YH and MS carried out the molecular genetic studies. YN, MN, SM, YM, and YH participated in the design of the study. All authors contributed to data analysis, interpretation, and final approval of the manuscript.

Acknowledgements

This work was supported by JSPS KAKENHI Grant Number 25462615, the Jikei Research Fund, and the Jikei graduate school Research Fund.

Author details

[1]Department of Obstetrics and Gynecology, The Jikei University School of Medicine, 3-25-8, Nishi-Shinbashi, Minato-ku, Tokyo 105-8461, Japan. [2]Department of Molecular Biology, The Jikei University School of Medicine, 3-25-8, Nishi-Shinbashi, Minato-ku, Tokyo 105-8461, Japan. [3]Division of Molecular Epidemiology, The Jikei University School of Medicine, 3-25-8, Nishi-Shinbashi, Minato-ku, Tokyo 105-8461, Japan.

Received: 1 September 2014 Accepted: 22 October 2014
Published: 3 November 2014

References

1. Takano M, Kikuchi Y, Yaegashi N, Kuzuya K, Ueki M, Tsuda H, Suzuki M, Kigawa J, Takeuchi S, Tsuda H, Moriya T, Sugiyama T: **Clear cell carcinoma of the ovary: a retrospective multicentre experience of 254 patients with complete surgical staging.** *Br J Cancer* 2006, **94:**1369–1374.
2. Nishimura S, Tsuda H, Ito K, Takano M, Terai Y, Jobo T, Kigawa J, Sugiyama T, Yaegashi N, Aoki D: **Differential expression of hypoxia-inducible protein 2 among different histological types of epithelial ovarian cancer and in clear cell adenocarcinomas.** *Int J Gynecol Cancer* 2010, **20:**220–226.
3. Higashiura Y, Kajihara H, Shigetomi H, Kobayashi H: **Identification of multiple pathways involved in the malignant transformation of endometriosis (Review).** *Oncol Lett* 2012, **4:**3–9.
4. Tan DS, Kaye S: **Ovarian clear cell adenocarcinoma: a continuing enigma.** *J Clin Pathol* 2007, **60:**355–360.
5. Yokota N, Koizume S, Miyagi E, Hirahara F, Nakamura Y, Kikuchi K, Ruf W, Sakuma Y, Tsuchiya E, Miyagi Y: **Self-production of tissue factor-coagulation factor VII complex by ovarian cancer cells.** *Br J Cancer* 2009, **101:**2023–2029.
6. Lee YY, Kim TJ, Kim MJ, Kim HJ, Song T, Kim MK, Choi CH, Lee JW, Bae DS, Kim BG: **Prognosis of ovarian clear cell carcinoma compared to other histological subtypes: a meta-analysis.** *Gynecol Oncol* 2011, **122:**541–547.
7. Jones S, Wang TL, Shih IM, Mao TL, Nakayama K, Roden R, Glas R, Slamon D, Diaz LA Jr, Vogelstein B, Kinzler KW, Velculescu VE, Papadopoulos N: **Frequent mutations of chromatin remodeling gene ARID1A in ovarian clear cell carcinoma.** *Science* 2010, **330:**228–231.
8. Tsuchiya A, Sakamoto M, Yasuda J, Chuma M, Ohta T, Ohki M, Yasugi T, Taketani Y, Hirohashi S: **Expression profiling in ovarian clear cell carcinoma: identification of hepatocyte nuclear factor-1 beta as a molecular marker and a possible molecular target for therapy of ovarian clear cell carcinoma.** *Am J Pathol* 2003, **163:**2503–2512.
9. Hirasawa A, Saito-Ohara F, Inoue J, Aoki D, Susumu N, Yokoyama T, Nozawa S, Inazawa J, Imoto I: **Association of 17q21-q24 gain in ovarian clear cell adenocarcinomas with poor prognosis and identification of PPM1D and APPBP2 as likely amplification targets.** *Clin Cancer Res* 2003, **9:**1995–2004.
10. Tan DS, Lambros MB, Rayter S, Natrajan R, Vatcheva R, Gao Q, Marchiò C, Geyer FC, Savage K, Parry S, Fenwick K, Tamber N, Mackay A, Dexter T, Jameson C, McCluggage WG, Williams A, Graham A, Faratian D, El-Bahrawy M, Paige AJ, Gabra H, Gore ME, Zvelebil M, Lord CJ, Kaye SB, Ashworth A, Reis-Filho JS: **PPM1D is a potential therapeutic target in ovarian clear cell carcinomas.** *Clin Cancer Res* 2001, **15:**2269–2280.
11. Anglesio MS, George J, Kulbe H, Friedlander M, Rischin D, Lemech C, Power J, Coward J, Cowin PA, House CM, Chakravarty P, Gorringe KL, Campbell IG, Australian Ovarian Cancer Study Group, Okamoto A, Birrer MJ, Huntsman DG, de Fazio A, Kalloger SE, Balkwill F, Gilks CB, Bowtell DD: **IL6-STAT3-HIF signaling and therapeutic response to the angiogenesis inhibitor sunitinib in ovarian clear cell cancer.** *Clin Cancer Res* 2011, **17:**2538–2548.
12. Lu J, Getz G, Miska EA, Alvarez-Saavedra E, Lamb J, Peck D, Sweet-Cordero A, Ebert BL, Mak RH, Ferrando AA, Downing JR, Jacks T, Horvitz HR, Golub TR: **MicroRNA expression profiles classify human cancers.** *Nature* 2005, **435:**834–838.

13. Yanaihara N, Harris CC: **MicroRNA Involvement in Human Cancers.** *Clin Chem* 2013, **59**:1811–1812.
14. Volinia S, Calin GA, Liu CG, Ambs S, Cimmino A, Petrocca F, Visone R, Iorio M, Roldo C, Ferracin M, Prueitt RL, Yanaihara N, Lanza G, Scarpa A, Vecchione A, Negrini M, Harris CC, Croce CM: **A microRNA expression signature of human solid tumors defines cancer gene targets.** *Proc Natl Acad Sci USA* 2006, **103**:2257–2261.
15. Meng F, Henson R, Wehbe-Janek H, Ghoshal K, Jacob ST, Patel T: **MicroRNA-21 regulates expression of the PTEN tumor suppressor gene in human hepatocellular cancer.** *Gastroenterology* 2007, **133**:647–658.
16. Ho CM, Lin MC, Huang SH, Huang CJ, Lai HC, Chien TY, Chang SF: **PTEN promoter methylation and LOH of 10q22-23 locus in PTEN expression of ovarian clear cell adenocarcinomas.** *Gynecol Oncol* 2009, **112**:307–313.
17. Hashiguchi Y, Tsuda H, Inoue T, Berkowitz RS, Mok SC: **PTEN expression in clear cell adenocarcinoma of the ovary.** *Gynecol Oncol* 2006, **101**:71–75.
18. Tan DS, Iravani M, McCluggage WG, Lambros MB, Milanezi F, Mackay A, Gourley C, Geyer FC, Vatcheva R, Millar J, Thomas K, Natrajan R, Savage K, Fenwick K, Williams A, Jameson C, El-Bahrawy M, Gore ME, Gabra H, Kaye SB, Ashworth A, Reis-Filho JS: **Genomic analysis reveals the molecular heterogeneity of ovarian clear cell carcinomas.** *Clin Cancer Res* 2011, **17**:1521–1534.
19. Suehiro Y, Sakamoto M, Umayahara K, Iwabuchi H, Sakamoto H, Tanaka N, Takeshima N, Yamauchi K, Hasumi K, Akiya T, Sakunaga H, Muroya T, Numa F, Kato H, Tenjin Y, Sugishita T: **Genetic aberrations detected by comparative genomic hybridization in ovarian clear cell adenocarcinomas.** *Oncology* 2000, **59**:50–56.
20. Kuo KT, Mao TL, Chen X, Feng Y, Nakayama K, Wang Y, Glas R, Ma MJ, Kurman RJ, Shih IM, Wang TL: **DNA copy numbers profiles in affinity-purified ovarian clear cell carcinoma.** *Clin Cancer Res* 2010, **16**:1997–2008.
21. Calin GA, Sevignani C, Dumitru CD, Hyslop T, Noch E, Yendamuri S, Shimizu M, Rattan S, Bullrich F, Negrini M, Croce CM: **Human microRNA genes are frequently located at fragile sites and genomic regions involved in cancers.** *Proc Natl Acad Sci USA* 2004, **101**:2999–3004.
22. Yanaihara N, Caplen N, Bowman E, Seike M, Kumamoto K, Yi M, Stephens RM, Okamoto A, Yokota J, Tanaka T, Calin GA, Liu CG, Croce CM, Harris CC: **Unique microRNA molecular profiles in lung cancer diagnosis and prognosis.** *Cancer Cell* 2006, **9**:189–198.
23. Lindsey E, Becker B, Yong L: **Apoptosis and the target genes of miR-21.** *Chin J Cancer* 2011, **30**:371–380.
24. Zhang S, Dihua Y: **PI (3) King Apart PTEN's Role in Cancer.** *Clin Cancer Res* 2010, **16**:4325–4330.
25. Michaud DS, Daugherty SE, Berndt SI, Platz EA, Yeager M, Crawford ED, Hsing A, Huang WY, Hayes RB: **Genetic polymorphisms of interleukin-1B (IL-1B), IL-6, IL-8, and IL-10 and risk of prostate cancer.** *Cancer Res* 2006, **66**:4525–4530.
26. Yanaihara N, Anglesio MS, Ochiai K, Hirata Y, Saito M, Nagata C, Iida Y, Takakura S, Yamada K, Tanaka T, Okamoto A: **Cytokine gene expression signature in ovarian clear cell carcinoma.** *Int J Oncol* 2012, **41**:1094–10100.
27. Iliopoulos D, Jaeger SA, Hirsch HA, Bulyk ML, Struhl K: **STAT3 activation of miR-21 and miR-181b-1 via PTEN and CYLD are part of the epigenetic switch linking inflammation to cancer.** *Mol Cell* 2010, **39**:493–506.

doi:10.1186/1471-2407-14-799
Cite this article as: Hirata *et al.*: MicroRNA-21 is a candidate driver gene for 17q23-25 amplification in ovarian clear cell carcinoma. *BMC Cancer* 2014 14:799.

Arch Gynecol Obstet
DOI 10.1007/s00404-014-3446-7

GYNECOLOGIC ONCOLOGY

Success rate and safety of tumor debulking with diaphragmatic surgery for advanced epithelial ovarian cancer and peritoneal cancer

Motoaki Saitou · Yasushi Iida · Hiromi Komazaki · Chikage Narui · Kanae Matsuno · Ayako Kawabata · Kazu Ueda · Hiroshi Tanabe · Satoshi Takakura · Seiji Isonishi · Hiroshi Sasaki · Aikou Okamoto

Received: 28 March 2014 / Accepted: 26 August 2014

Abstract
Purpose In advanced epithelial ovarian and peritoneal cancer, residual tumor diameter correlates with prognosis; therefore, maximum debulking and optimal surgery (OS) for residual tumors <1 cm is warranted. Here, we clarified the efficacy of tumor debulking with diaphragmatic surgery (DS).
Methods In 45 patients with epithelial ovarian or peritoneal cancer who underwent DS (ten, full-thickness resection; 35, stripping) between January 2010 and December 2013 at two related institutions, we retrospectively evaluated OS safety and success by surgical duration, blood loss, complications, hospitalization stay, and residual tumor diameter and site.
Results Blood loss was 4,090.8 and 2,847.9 mL; surgical duration was 485.2 and 479.5 min; hospitalization stay was 21.7 and 24.8 days; and complications included intraoperative thoracotomy in 17 and 7 patients, unexpected thoracotomy in 11 and 3, chest drain insertion in one and three, and pleural effusion in 14 and 7, in the primary debulking surgery (PDS) and interval debulking surgery (IDS) groups, respectively. OS was successful in all patients with complete surgery (CS: no residual tumor) achieved in 16 (50.0 %) and 9 (69.2 %), residual tumor diameter < 5 mm in 11 (34.4 %) and 2 (15.4 %), and residual tumor diameter < 1 cm in 5 (15.6 %) and 2 (15.4 %) in the PDS and IDS groups, respectively.
Conclusions Tumor debulking surgery with DS resulted in controllable blood loss, and OS was successful in all patients without severe complications or postoperative treatment delay. Currently, OS is considered to have very few benefits over CS; thus, the success rate of CS rate should be improved while maintaining safety.

Keywords Ovarian cancer · Diaphragmatic surgery · Debulking surgery · Peritoneal cancer

Introduction

Ovarian cancer has few subjective symptoms. Consequently, at present, approximately 40–50 % of cases are detected in advanced stages (III/IV), which may be attributed to the difficulty in early detection and mass screening. As a result, of all gynecologic malignancies, ovarian cancer has the highest mortality. Although the advent of paclitaxel has improved therapeutic outcomes of ovarian cancer, the 5-year survival rate of advanced cases remains low (25–37 %) and typically require multimodal therapeutic combinations of surgery and chemotherapy.

The first-line treatment of ovarian cancer is surgery, which generally involves bilateral salpingo-oophorectomy, total hysterectomy, and omentectomy. Staging by laparotomy is required to determine disease stage and involves intraperitoneal cytodiagnosis, intraperitoneal biopsy, and radical dissection (biopsy) of the retroperitoneal (pelvic and para-aortic) lymph nodes.

The prognostic factors of ovarian cancer include staging, histologic type, and residual tumor diameter after primary debulking surgery (PDS). Residual tumor diameter is considered a particularly important factor. Surgery, such as resection of disseminated and metastatic lesions, is

M. Saitou (✉) · Y. Iida · H. Komazaki · C. Narui · K. Matsuno · A. Kawabata · K. Ueda · H. Tanabe · S. Takakura · S. Isonishi · H. Sasaki · A. Okamoto
Department of Obstetrics/Gynecology,
Jikei University School of Medicine, 3-25-8 Nishi-shinbashi,
Minato-Ku, Tokyo 105, Japan
e-mail: smotoaki@jikei.ac.jp

Published online: 04 September 2014

performed so that the margin of the residual tumor is as close to zero as possible. Tumor debulking surgery is generally performed as a first-line treatment, even in stage IV cases with distal metastasis, excluding those in which distal metastasis impacts short-term survival. Prognosis is improved when the residual tumor diameter is <1 cm, in which case surgery is referred to as optimal surgery (OS). Therefore, the standard treatment for advanced ovarian cancer at the time of primary surgery is maximum debulking surgery followed by chemotherapy. However, views on OS have changed in recent years. In 2009, Du Bois et al. [1] reported that other than reducing the size of the residual tumor, OS offers very few benefits to patients with advanced ovarian cancer (stage IIb or greater). In our facilities, we recently adopted diaphragmatic surgery (DS) as a part of OS. Nonetheless, we currently aim for complete surgery (CS) for cases of advanced ovarian cancer.

Patients and methods

In the present study, we examined 45 patients with epithelial ovarian cancer or peritoneal cancer who underwent tumor debulking with DS at two related institutions between January 2010 and December 2013. All patients underwent standard surgical procedures (bilateral salpingo-oophorectomy, total hysterectomy, or omentectomy) and retroperitoneal lymph node dissection (biopsy), in addition to DS (stripping and full-thickness resection). The procedure of diaphragmatic stripping conducted at our hospital is as follows. To ensure an adequate field of view, images of the state of liver mobilization (Fig. 1a) are obtained, after which, diaphragmatic stripping (Fig. 1b) is performed. At this point, the liver is fixed which requires approximately 10–15 min. Soon after fixation, blood flow is resumed and surgery is continued. In cases undergoing diaphragm full-thickness resection (Fig. 2), the diaphragm is reconstructed (Fig. 2, 3) using absorbable sutures (PDS in our hospital). Thereafter, deflation is performed using a narrow tube (Fig. 3) at our institution (20 G; BD Insyte Autoguard Shielded IV Catheter; Becton–Dickinson, Tokyo, Japan) and the chest is closed. Finally, a bubble test is performed under positive pressure ventilation to confirm sufficient airtight chest closure. Furthermore, for all patients, post-operative chest radiography is performed in the operating room to confirm the absence of pneumothorax.

Results

The subject cohort comprised 45 patients (mean age, 53 years), including 41 with ovarian cancer and four with peritoneal cancer. The histological types included serous adenocarcinoma ($n = 31$), endometrioid adenocarcinoma ($n = 4$), clear cell adenocarcinoma ($n = 6$), mixed-type ($n = 3$), and others ($n = 1$). With respect to staging, two patients had stage IIIb disease, 33 had stage IIIc, and 10 had stage IV. With respect to the type of surgery, PDS was performed in 32 cases and interval debulking surgery (IDS) in 13 (Table 1). In the PDS and IDS groups, the mean blood loss volume was 4,090.8 and 2,847.9 mL, and the mean surgical duration was 485.2 and 479.5 min, respectively. Stripping was performed in 26 and 9 patients, and full-thickness resection was performed in six and four patients, respectively. Complications included intraoperative thoracotomy in 17 and 7, unexpected thoracotomy in 11 and 3, chest drain insertion in one and three, and postoperative pleural effusion in 14 and 7 patients, respectively. The mean length of hospitalization was 21.7 and 24.8 days, respectively. OS was successfully completed in all patients. In the PDS and IDS groups, CS was achieved (CS: no residual tumor) in 16 (50 %) and 9 (69.2 %) patients, and the residual tumor diameter was<5 mm in 11 (34.4 %) and 2 (15.4 %) patients and

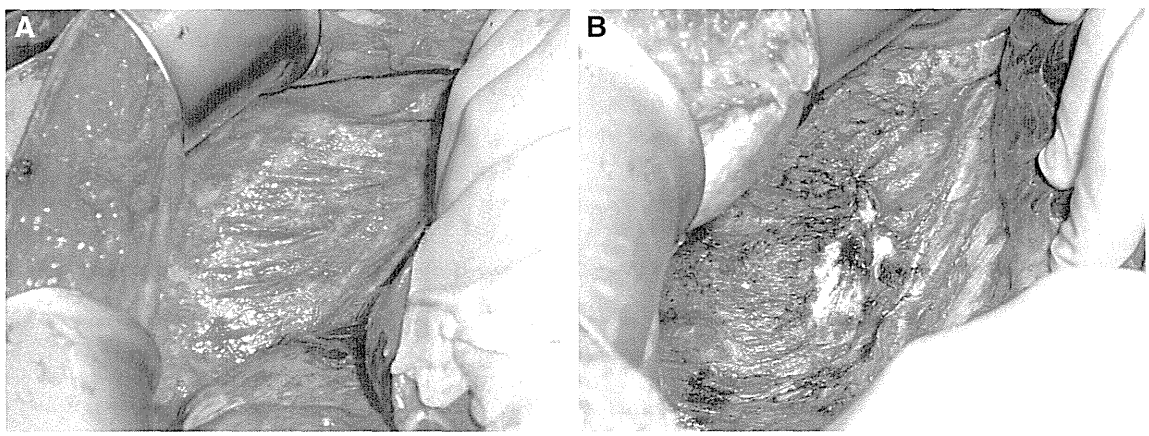

Fig. 1 **a** Diaphragm disease. **b** Diaphragmatic stripping is performed

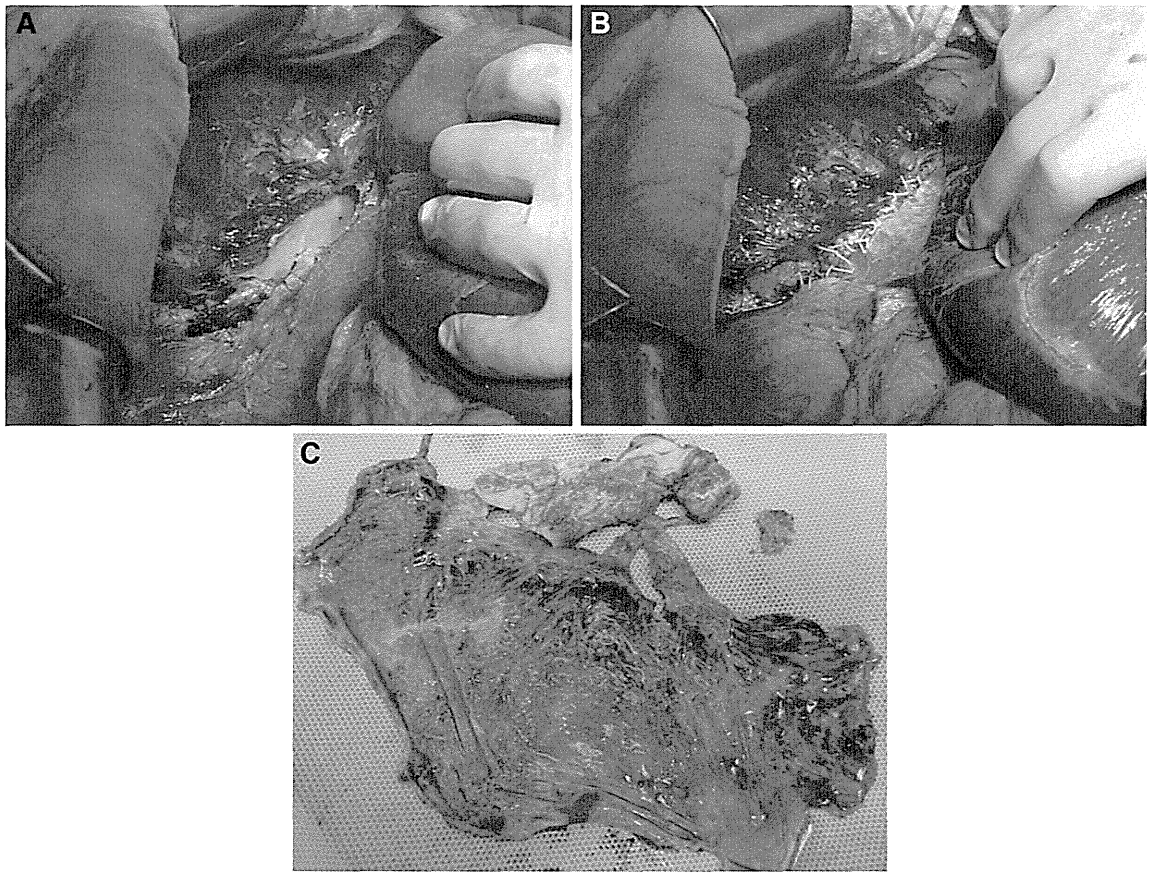

Fig. 2 **a** Diaphragm full-thickness resection completed. **b** The diaphragm is reconstructed using absorbable sutures. **c** This is a resected disease from the right diaphragm

<1 cm in five (15.6 %) and two (15.4 %) patients, respectively. The residual tumor site included the diaphragm, liver surface, mesentery, splenic hilum, and peritoneum (Table 2).

Discussion

When PDS for ovarian and/or peritoneal cancer is performed, it is important to accurately determine staging (surgical staging) based on systematic intraperitoneal tests and minimize the residual tumor to determine an appropriate treatment modality to improve prognosis. In recent years, opinions regarding optimal surgery have changed drastically. In our facilities, we recently adopted DS as a part of OS, although CS has been typically planned with DS since 2009.

With regard to the history of OS and CS, in 1994, Hoskins et al. [2] reported a correlation between residual tumor diameter and prognosis in primary laparotomy. Since then, the importance of primary laparotomy has been debated, and in 2002, Bristow et al. [3] performed a meta-analysis and concluded that for patients with stage III/IV ovarian carcinoma, tumor debulking is the most important factor impacting survival. However, this study provides the only evidence of surgery for advanced ovarian cancer, in which a residual tumor with a diameter of <1 cm indicated a significantly good prognosis and was considered for OS, which may be used as a target in primary surgery. In 2006, Chi et al. [4] divided 465 patients with stage IIIc ovarian cancer into five groups according to residual tumor diameter and comparatively examined patient prognosis. Similar to current reports, comparing patients with a residual tumor diameter of <1 vs. >1 cm, the former group had significantly better prognosis. Moreover, a significant difference in survival was found between patients without residual tumors and those with a residual tumor of <1 cm. These results may mark the beginning of a shift toward CS in primary laparotomy. Furthermore, IDS should be performed in cases in which chemotherapy following PDS reduces the tumor by more than 50 %. In cases with stable or progressive disease, IDS is contraindicated because it may worsen prognosis. When IDS is performed, CS should be targeted; however, as with PDS, it is important to

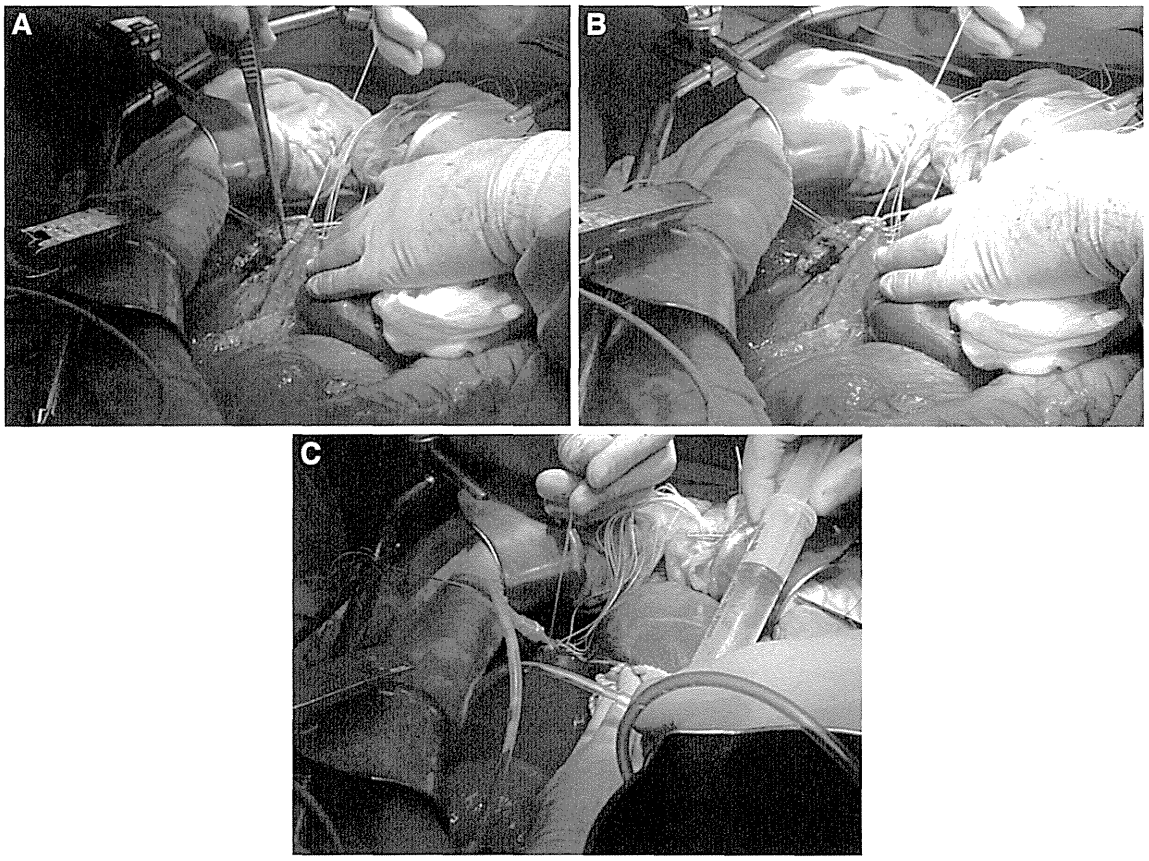

Fig. 3 **a**, **b** The diaphragm is reconstructed using absorbable sutures. **c** Deflation is performed using a narrow tube

choose the optimal surgical procedure for each patient. Qayyum et al. [5] reported that sites of tumor metastasis may impede CS (Table 3). In our study, unfortunately, we also found residual tumors in the diaphragm, mesentery, splenic hilum, and peritoneum as well as on the liver surface. We believe that the choice of a surgical procedure for cases with residual tumors and the ability to quickly and accurately intraoperatively determine the extent to which surgery should be performed needs to be addressed in the future.

Subsequently, metastatic dissemination in the diaphragm is observed in approximately 40 % or more of patients with advanced ovarian cancer. Zivanovic et al. [6] reported that the presence of metastatic epigastric lesions in ovarian cancer was significantly correlated with excessive accumulation of ascites and suboptimal cytoreduction. Moreover, in cases in which epigastric lesions may be managed by optimal cytoreduction, the recurrence risk is reportedly reduced to 28 % and the risk of death to 33 % [7]. Therefore, CS may help control the development of epigastric lesions.

Although many recent reports have described the safety and usefulness of surgical procedures, such as stripping and full-thickness resection, in many cases, it is difficult to remove lesions that have disseminated throughout the diaphragm. In such instances, extensive lesions may fill the right triangular ligament of the diaphragm bordering the liver. Therefore, we recommend diaphragmatic stripping or diaphragmatic resection in such cases, although extensive diaphragmatic resection in cases with diaphragmatic permeation should be limited. Moreover, in cases that without extensive diaphragmatic permeation, diaphragmatic reconstruction is performed without soft tissue patch (GORE-TEX; W.L.Go re & Associates, Inc.,Tokyo, Japan) use in our hospital. Intraoperative procedural accidents include unexpected thoracotomy during stripping, whereas postoperative complications include pleural effusion. Terauchi et al. [8] reported that the incidence of unexpected thoracotomy and pleural effusion was 1.6 and 30.8 %, and 52.3 and 61.5 % in the PDS and IDS groups, respectively. At our hospital, unexpected thoracotomy occurred in 42.3 and 33.3 %, and pleural effusion in 43.8 and 53.8 %, in the PDS and IDS groups, respectively. Unexpected thoracotomy was common in the IDS group, which may be because of tissue fibrosis caused by the use of anticancer agents. The results at our hospital revealed that nearly half (42.3 %) of the patients in the PDS group required thoracotomy, which unfortunately may be considered resultant

Table 1 Patient characteristics

Characteristics	No. of patients	% of 45 patients
Age		
Mean age (years)	52.7	
Range	(37–73)	
Primary cancer		
Ovary	41	91.1
Peritoneal	4	8.9
Histological type		
Serous	31	68.9
Endometrioid	4	8.9
Clear	6	13.3
Mucinous	0	0
Mixed	3	6.7
Other	1	2.2
Stage		
IIIb	2	4.4
IIIc	33	73.3
IV	10	22.2
Surgical method		
PDS	32	71.1
IDS	13	28.9

PDS primary debulking surgery, *IDS* interval debulking surgery

Table 2 Intra- and post-operative data on DS

	PDS	IDS
Number of patients	32	13
Diaphragmatic surgery		
Stripping (%)	26 (81.3)	9 (62.2)
Full-thickness resection (%)	6 (18.8)	4 (30.8)
Intraoperative open chest (%)	17 (53.1)	7 (53.8)
Unexpected open chest (%)	11 (42.3 %)	3 (33.3 %)
Postoperative pleural effusions (%)	14 (43.8)	7 (53.8)
Pneumothorax (%)	0	0
Chest tube (%)	1 (3.1)	3 (23.1)
Side of diaphragmatic disease		
Right (%)	27 (84.3)	12 (92.3)
Bilateral (%)	5 (15.6)	1 (7.7)
Complete cytoreduction (%)		
Macroscopic residual tumor		
None	16 (50.0)	9 (69.2)
<5 mm	11 (34.4)	2 (15.4)
	Porta hepatis	Mesentery
	Mesentery	Small bowel mesentery
	Peritoneum	
<10 mm	5 (15.6)	2 (15.4)
	Lymphnode (PAN)	Liver surface
		Mesentery
	Diaphragm	
Mean intraoperative blood loss (mL)	4,090.8	2,847.9
Mean duration of the operation (min)	485.2	479.5
Mean hospitalization (days)	21.6	24.8

PDS primary debulking surgery, *IDS* interval debulking surgery

Table 3 Criteria for inoperable disease in newly diagnosed primary epithelial ovarian cancer

Peritoneal sites	Nodal sites	Other
Porta hepatis	Retroperitoneal	Hepatic metastases
Intersegmental fisure	(Above the renal hila)	Abdominal wall invasion
Subphrenic space	Celiac axis	
Gastrosplenic ligament	Supradiaphragmatic	
Lesser sac		
Small bowel mesentery		
Dome of the liver surface		

Aliya Qayyum et al. [5]

of competency. With respect to pleural effusion, there was no considerable difference between the two groups. Furthermore, Tsolakidis et al. [9] reported no residual tumor in 88.7 % of the PDS group and 94.6 % of the IDS group, which were relatively high rates. The blood loss volume, surgical duration, and length of hospitalization until aftercare in the PDS group were 2,177 mL, 355 min, and 21 days, respectively; in the IDS group, these values were 1,270 mL, 272 min, and 13 days, respectively. Among our patients, the values for complete cytoreduction were relatively low at 50.0 and 69.2 %, respectively. The blood loss volume, surgical duration, and length of hospitalization until aftercare in the PDS group were 4,091 mL, 485 min, and 21 days, respectively; in the IDS group, these values were 2,848 mL, 480 min, and 25 days, respectively. There were no significant differences observed other than the length of hospitalization in the PDS group. Beginning in 2009, only 5 years ago, many Japanese medical institutions adopted DS; therefore, major differences in complications, surgical duration, and blood loss volume may be attributed to inexperience. Because of the long learning curve due to the prolonged duration for legal approval of the epigastric method before it was applied to the diaphragmatic approach for liver surgery, the amount of blood loss associated with this procedure has continued to increase. In addition, switching to an open chest procedure was required in some cases, and several cases had postoperative hydrothorax. Moreover, the time from start of therapy and length of stay has increased.

Conclusions

The most important factor to establish a treatment plan for advanced cancer at the time of primary laparotomy and IDS is the extent to which a residual tumor can be eradicated. However, successful CS is dependent on patient age, performance status, and the presence or absence of complications. We believe that surgery should always be performed aiming for CS and should not markedly reduce the patient's quality of life. At our hospital, tumor debulking with DS resulted in excessive, but controllable blood loss, and OS was safely and successfully achieved in all patients, without any severe complications or delay in postoperative treatment. In 2009, du Bois et al. [1] reported that OS was considered to have very few benefits over CS; therefore, the success rate of CS should be improved while maintaining safety and, at the same time, gynecologic oncologists should improve their skills in surgical repair of the epigastric region.

Conflict of interest None.

References

1. Du Bois A, Reuss A, Pujade-Lauraine E, Harter P, Ray-Coquard I, Pfisterer J (2009) Role of surgical outcome as prognostic factor in advanced epithelial ovarian cancer: a combined exploratory analysis of 3 prospectively randomized phase 3 multicenter trials: by the Arbeitsgemeinschaft Gynaekologische Onkologie Studiengruppe Ovarialkarzinom (AGO-OVAR) and the Groupe d'Investigateurs Nationaux Pour les Etudes des Cancers de l'Ovaire (GINECO). Cancer 115:1234–1244. doi:10.1002/cncr.24149
2. Hoskins WJ, McGuire WP, Brady MF, Homesley HD, Creasman WT, Berman M, Ball H, Berek JS (1994) The effect of diameter of largest residual disease on survival after primary cytoreductive surgery in patients with suboptimal residual epithelial ovarian carcinoma. Am J Obstet Gynecol 170:974–980
3. Bristow RE, Tomacruz RS, Armstrong DK, Trrimble EL, Montz FJ (2002) Survival effect of maximal cytoreductive surgery for advanced ovarian carcinoma during the platinum era: a meta-analysis. J Clin Oncol 20:1248–1259
4. Chi DS, Eisenhauer EL, Lang J, Huh J, Haddad L, Abu-Rustum NR, Sonoda Y, Levine DA, Hensley M, Barakat RR (2006) What is the optimal goal of primary cytoreductive surgery for bulky stage IIIC epithelial ovarian carcinoma (EOC)? Gynecol Oncol 103:559–564
5. Qayyum A, Coakley FV, Westphalen AC, Hricak H, Okuno WT, Powell B (2005) Role of CT and MR imaging in predicting optimal cytoreduction of newly diagnosed primary epithelial ovarian cancer. Gynecol Oncol 96:301–306
6. Zivanovic O, Eisenhauer EL, Zhou Q, Iasonos A, Sabbatini P, Sonoda Y, Abu-Rustum NR, Barakat RR, Chi DS (2008) The impact of bulky upper abdominal disease cephalad to the greater omentum on surgical outcome for stage IIIC epithelial ovarian, fallopian tube, and primary peritoneal cancer. Gynecol Oncol 108:287–292
7. Zivanovic O, Sima CS, Iasonos A, Hoskins WJ, Pingle PR, Leitao MM Jr, Sonoda Y, Abu-Rustum NR, Barakat RR, Chi DS (2010) The effect of primary cytoreduction on outcomes of patients with FIGO stage IIIC ovarian cancer stratified by the initial tumor burden in the upper abdomen cephalad to the greater omentum. Gynecol Oncol 116:351–357. doi:10.1016/j.ygyno.2009.11.022
8. Terauchi F, Okamoto A, Wada Y, Hasegawa E, Sasaki T, Akutagawa O, Sagawa Y, Nishi H, Isaka K (2010) Incidental events of diaphragmatic surgery in 82 patients with advanced ovarian, primary peritoneal and fallopian tubal cancer. Oncol Lett 1:861–864. doi:10.3892/ol_00000152
9. Tsolakidis D, Amant F, Leunen K, Cadron I, Neven P, Vergote I (2011) Comparison of diaphragmatic surgery at primary or interval debulking in advanced ovarian carcinoma: an analysis of 163 patients. Eur J Cancer 47:191–198. doi:10.1016/j.ejca.2010.08.020

Uterine endometrial carcinoma with trophoblastic differentiation: a case report with literature review

T. Seki[1], N. Yanaihara[1], Y. Hirata[1], M. Fukunaga[2], T. Tanaka[1], A. Okamoto[1]

[1]Department of Obstetrics and Gynecology
[2]Department of Pathology, The Jikei University School of Medicine, Minato-ku, Tokyo (Japan)

Summary

Choriocarcinoma is categorized as either gestational or nongestational depending on its origin. Nongestational choriocarcinoma originated in the trophoblastic differentiation is a rare but an aggressive tumor. This article reports a nongestational case of a uterine endometrial carcinoma with trophoblastic differentiation. A 54-year-old woman with a history of atypical genital bleeding that underwent semi-radical hysterectomy, bilateral salpingo-oophrectomy, and pelvic lymph nodes dissection. Pathological investigation showed that the tumor had endometrioid adenocarcinoma and choriocarcinomatous components. Although a series of multimodality treatments including craniotomy were performed, she died of aggressive lung and brain metastases one year after the primary surgery.

Key words: Nongestational choriocarcinoma; Endometrial carcinoma; Trophoblastic differentiation.

Introduction

Gestational trophoblastic diseases, characterized by abnormal proliferation of pregnancy-associated trophoblastic tissues, include a range of rare disorders such as hydatidiform moles, invasive moles, and choriocarcinoma. Choriocarcinoma is a highly malignant tumor and is categorized as either gestational or nongestational. Gestational choriocarcinoma can occur preceding any gestational event. A few choriocarcinomas called nongestational choriocarcinoma are independent of the gestational events and arise from the trophoblastic differentiation of germ cell tumor and carcinoma, or residual germ cell. The authors describe here a rare case of uterine endometrial carcinoma with trophoblastic differentiation, while reviewing pertinent literature.

Case Report

A 54-year-old woman (gravida2, para2) came to the present gynecologic department with postmenopausal atypical genital bleeding. Pelvic examination revealed a large uterine mass and transvaginal ultrasonography showed the enlarged uterus of 12 × 8 cm and irregular thickness in the endometrium (Figure 1a). Endometrial biopsy revealed endometrioid adenocarcinoma (grade 1). Pelvic magnetic resonance imaging (MRI) showed a solid bulky mass, filling the uterine cavity, and infiltrating the uterine wall (Figure 1b), and chest computed tomography (CT) showed multiple lung nodules suggesting lung metastases (Figure 1c). The patient underwent semi-radical hysterectomy, bilateral salpingo-oophrectomy, and pelvic lymph nodes dissection.

Pathological examination revealed a mass 14×80×55 mm in size (Figure 2a) was in the uterine cavity. The tumor extended to the cervix, penetrating greater than 50% of the myometrium and spreading to the right ovary and Douglas peritoneum. Microscopically, there were two different histological types of tumor in the specimen; namely, 95% of the tumor showed poorly differentiated endometrioid adenocarcinoma and the remaining part showed extensive hemorrhage and necrosis (Figure 2b). This remaining portion consisted of multinucleated giant cells showing a sporadic/focal pattern and eosinophilic cytoplasm resembling syncytiotrophoblastic cells, and other cells showing oval nuclear and pale cytoplasm resembling cytotrophoblastic cells (Figure 2c). In addition, the immunohistochemistry stain for human chorionic gonadotropin–β (hCG-β) (Figure 2d), human placenta lactogen (hPL), and inhibin-α turned out to be positive; therefore, this part is thought to exhibit the trophoblastic feature. Although the preoperative serum hCG level was not measured, the postoperative serum hCG level was elevated to 1,632 mIU/ml. Finally, the patient was diagnosed as having endometrioid adenocarcinoma with trophoblastic differentiation of uterine corpus and classified as International Federation of Gynecology and Obstetrics (FIGO) Stage IVb (pT3aN0M1).

The patient started to receive tri-weekly AP (doxorubicin, 60 mg/m^2; CDDP, 50 mg/ m^2) chemotherapy. Since metastatic lung tumors were enlarged (Figure 2b) with elevated serum hCG (8,318 mIU/ml) after three cycles of AP, the regimen was changed to MEA (methotrexate, 450 mg/body, day 1; etoposide, 100 mg/body, days 1–5; actinomycin D, 0.5 mg/body, days 1–5). Three cycles of MEA regimen could reduce the size of lung metastatic lesions (Figure 1d) as well as serum hCG value (291 mIU/ml). However, CT image again revealed increased number of lung metastatic lesions (Figure 1e) and new metastatic lesion appeared in the left occipital lobe of brain after five cycles of MEA. Craniotomy was performed to remove the metastatic brain tumor and pathological diagnosis of the tumor was pure choriocarcinoma. Soon after the craniotomy, another brain metastatic lesion was found and the patient died one year after primary surgery.

Discussion

Based on the information obtained from clinical observations, histopathological facts, and genetic origin, choriocarcinoma is categorized as gestational or nongestational. In

Revised manuscript accepted for publication July 23, 2013

Eur. J. Gynaec. Oncol. - ISSN: 0392-2936
XXXV, n. 4, 2014
doi: 10.12892/ejgo24642014

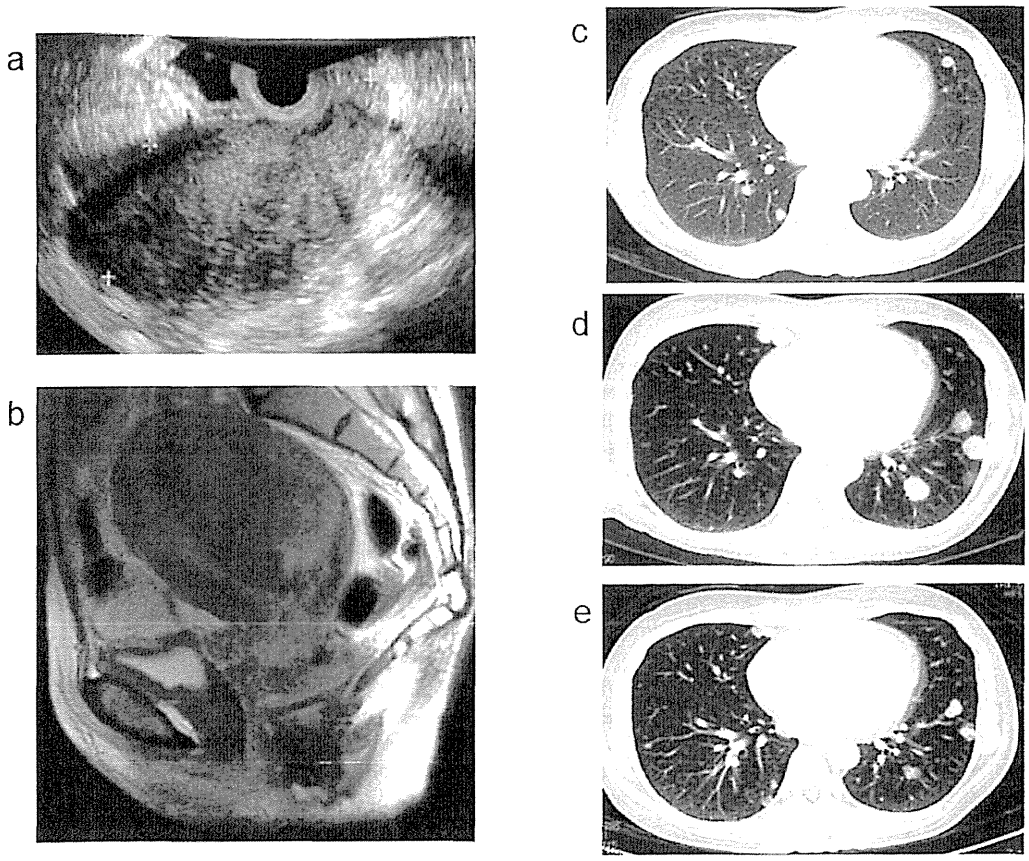

Figure 1. — Imaging studies. (a) Transvaginal ultrasound examination of enlarged uterus. (b) Pelvic magnetic resonance imaging (MRI) showing a solid bulky mass measured about 12 cm, filling the uterine cavity and infiltrating the uterine wall. (c) Chest computed tomography (CT) of lung field showing multiple lung metastasis before primary surgery. (d) Lung metastatic regions were enlarged after three cycles of AP treatment. (e) Lung metastatic regions were reduced after three cycles of MEA treatment.

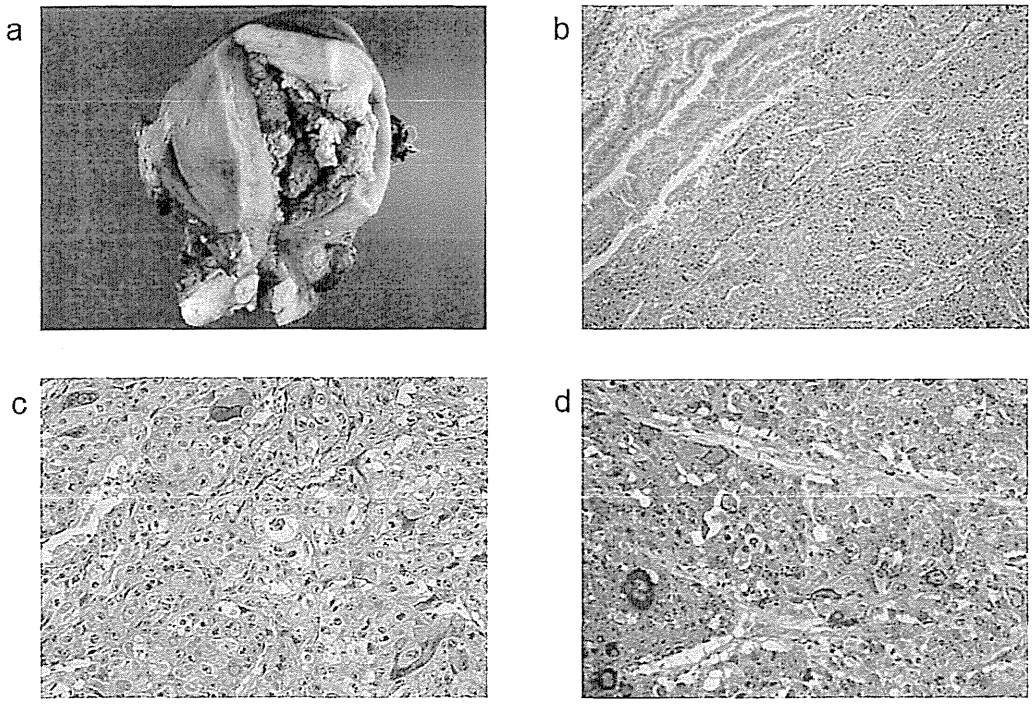

Figure 2. — Pathological findings. (a) Gross picture showing yellowish and white tumor occupying the endometrial cavity. (b) Histological examination showing the tumor composed of poorly differentiated adenocarcinoma (left upper) and choriocarcinoma (right) (HE×100). (c) The choriocarcinomatous component is characterized by a sheet of both proliferative cytotrophoblasts and syncytiotrophoblasts (HE×250). (d) Syncytiotrophoblasts were positive for hCG-β immunostaining (×250).

Table 1. — *Cases of uterine endometrial carcinoma with trophoblastic differentiation.*

Author	Age	G/P	Area of choriocarcinoma component	Coexisting tumor	Histology at metastasis or recurrence	Chemotherapy regimen	Metastasis region	Follow up (month)	Outcome
Civantos *et al.* [5]	87	3/2	ND	SA	ND	-	ND	ND	ND
Savage *et al.* [6]	70	1/1	Small area	Well EA	Choriocarcinoma	MPA, 5-FU+ DXR+megestrol acetate	brain, lung, kidney, liver	14	DOD
Pesce *et al.* [7]	78	ND/0	ND	Poor AC	ND	CDDP+BLM+ VCR	pelvic lymph node	1.5	DOD
	48	5/ND	ND	Poor AC	ND	MTX, BEP	lung	2	AWD
	63	MP/ND	ND	AC	Same as primary	-	lung, liver, peritoneum	14	DOD
Kalir *et al.* [8]	83	0/0	ND	Mod EA	ND	CDDP, etoposide	lung	1	AWD
Black *et al.* [9]	88	ND/1	ND	CCC		-	-	12	NED
Bradley *et al.* [10]	68	4/4	Focal area	Mixed	SA	PTX, CBDCA	pelvic lymph node	24	NED
Tunc *et al.* [11]	54	6/6	10-20%	Mod EA	AC	MEA, CPA+ folinic acid+ etoposide	retroperitoneum	24	DOD
Nguyen *et al.* [12]	34	0/0	Major area	MMMT	Choriocarcinoma	BEP, EMACO	brain, lung	4	AWD
Khuu *et al.* [13]	71	0/0	ND	Carcinosarcoma	-	-	-	8	NED
Horn *et al.* [14]	61	3/3	30%	SA	ND	MEA, EMACO	lung	3	DOD
Akbulut *et al.* [4]	42	ND	Small area	Mod EA	-		-	6	NED
Yamada *et al.* [15]	58	1/1	50%	Well EA	Choriocarcinoma	CBDCA, therarubicin, CPA, EMACO	vagina	45	NED
Olson et al. (3)	68	6/4	Focal area	EA	Choriocarcinoma	-	axillary lymph node	ND	ND
Present case	54	2/2	5%	Poor EA	Choriocarcinoma	DXR+CDDP, MEA	lung, brain	12	DOD

G/P: gravida/para; MP: multiparous; SA: serous adenocarcinoma; EA: endometrioid adenocarcinoma; AC: adenocarcinoma; CCC: clear cell adenocarcinoma; MMMT: malignant mixed mesodermal tumor; Mod: moderately differentiated; Poor, poorly differentiated; MPA: medroxyprogesterone; 5-FU: 5-fluorouracil; DXR: doxorubicin; CDDP: cispltin; BLM: bleomycin; VCR: vincristine; MTX: methotorexate; PTX: paclitaxel; CBDCA: carboplatin; CPA: cyclophosphamide; MEA: methotrexate+etoposide+actinomycin D; EMACO: etoposide+methotrexate+actinomycin D+cyclophosphamide+vincristin; NED: no evidence of the disease; AWD: alive with the disease; DOD: dead of the disease; ND: not described.

particular, nongestational choriocarcinoma is defined based primarily on the patient's reproductive history. Recently, DNA polymorphism analysis has been successfully utilized to identify the genetic origin of choriocarcinoma [1-2]. Although DNA analysis was not performed in the case in this report, the authors diagnosed it as nongestational choriocarcinoma because she also had endometrioid adenocarcinoma. Gestational choriocarcinoma is chemosensitive and the prognosis is good even in advanced stages. On the other hand, nongestational choriocarcinoma is less sensitive to chemotherapy and has a poor prognosis. Therefore, it is clinically important to determine the exact type of choriocarcinoma for identifying the appropriate treatment strategy.

Although three causes of nongestational trophoblastic tumor have been proposed, the pathogenesis of nongestational choriocarcinoma is still uncertain [3]. It is widely accepted that nongestational trophoblastic neoplasms might originate in either germ cell tumors or carcinomas as reported here. Recently, it has been reported that molecular genetic analysis showed a clonal evolution from endometrioid adenocarcinoma to trophoblastic tumor in a case of uterine endometrial adenocarcinoma with trophoblastic differentiation [3]. Thirdly, nongestational choriocarcinoma rarely has its origin in residual germ cells that could not migrate to the gonads without other neoplastic components [2].

Trophoblastic differentiation is histologically found in several types of tumors including stomach, lung, colon, esophagus, bladder, breast, and gynecologic cancers. Uterine endometrial carcinoma with trophoblastic differentiation is rare, and only a small number of cases have been reported so far [4]. The clinical characteristics of the tumor are its rapid growth, often at an advanced stage at the time of diagnosis, early metastases and poor prognosis, and therefore, identification of choriocarcinomatous component is thought to be important. Endometrial cancer with trophoblastic differentiation was first reported by Civantos and Rywlin in 1972 [5] and 16 cases have since been reported so far including the present case (Table 1) [3-15]. The mean age was 65.5 years (34-88) and 11 cases were multigravida. All cases showed abnormal genital bleeding and had high hCG levels in either serum or urine. In addition, immunohistochemical staining of hCG in the choriocarcinomatous element was found in all cases. As for the histology of the co-existing tumor, eight cases were endometrioid adenocarcinoma, three serous ade-